ISSN 1392-1320 MATERIALS SCIENCE (MEDŽIAGOTYRA). Vol. XX, No. X. 2025

Size and Shape Effect on Melting Temperature of Metallic Nanocrystals

Liqin ZHANG, Shitao XU *

Department of Physics and Electronic Information, Huaibei Normal University, Huaibei 235000, China

http://doi.org/10.5755/j02.ms.38032

Received 13 July 2024; accepted 12 September 2024

The melting temperature serves as a pivotal physical property governing the thermal stability of metallic nanocrystals, notably exhibiting substantial variability with respect to size and dimensionality. While several quantitative models exist to elucidate how the melting temperature correlates with the size and dimensionality of metallic nanocrystals, these models often fall short of capturing the synergistic influence of both factors comprehensively. To address this gap, our study employs a novel thermodynamic framework grounded in cohesive energy theory, requiring no arbitrary adjustable parameters. We find that, under constant conditions, the melting temperature of metallic nanocrystals diminishes as their size decreases. In terms of dimensionality, we establish a hierarchy as follows: nanoparticles > nanowires > thin films. Moreover, we reveal a non-linear relationship between the melting temperature and the inverse of dimensionality. Through rigorous validation via both simulations and empirical experiments, we corroborate the high accuracy of this thermodynamic model in predicting the variations in the melting temperature of metallic nanocrystals due to changes in size and dimensionality. The model in this study is primarily applicable to metallic nanocrystals and the potential applicability to other types of nanocrystals under certain conditions is briefly mentioned.

Keywords: melting temperature, cohesive energy, size effect, nanocrystals, thermodynamic model.

1. INTRODUCTION

Metallic nanocrystals (MNCs) have demonstrated immense application potential in various fields such as physics, biology, and chemistry due to their size-dependent properties [1 – 5]. Specifically, nanocrystals have found applications in catalysis, where their large surface area and tunable surface properties enhance catalytic reactions, making them highly effective for processes like hydrogen production and environmental remediation [6 – 8]. In biology, nanocrystals are used as highly sensitive biosensors due to their unique optical properties, enabling the detection of biomolecules at low concentrations [9, 10]. Additionally, in optoelectronics, nanocrystals contribute to the development of advanced light-emitting diodes (LEDs) and photovoltaic devices, where their size-dependent bandgap can be tuned to optimize performance [11, 12]. These specific applications highlight the versatile and transformative potential of nanocrystals across multiple scientific disciplines. In contrast to macroscopic materials, their high surface-to-volume ratio and surface structure reconstructions result in energy elevations and energy level rearrangements [6 – 11]. The low-dimensional characteristics of nanocrystals are especially evident in quantum confinement effects, surface states, and interfacial phenomena [12 – 22]. Thus, systematic investigation of the size-dependent properties of these low-dimensional materials at the nanoscale is crucial for understanding and developing the fundamental mechanisms of nanotechnology across its applications [23 – 30].

Among the various properties of MNCs, the melting point, T_m, stands out as a key thermodynamic parameter reflecting the thermal stability of the material across different sizes. Existing studies have observed that for certain metal nanocrystals, such as lead (Pb), tin (Sn), bismuth (Bi), and indium (In), the melting point decreases with decreasing size [31 – 36]. However, when these nanocrystals are embedded into other matrix materials, the melting point can exhibit complex dependency behaviors. For example, by using differential scanning calorimetry (DSC), the heating phenomenon of In and Pb embedded in Al matrixes and Pb nanofilms in Al matrixes observed the melting point increased with size decreasing [13, 14, 37, 38] Furthermore, when Pb nanofilms are sandwiched by Al layers, or in nanoparticles embedded in Al matrices, the melting temperatures of them are found either increased or decreased with the size decreasing [15 – 20, 39, 40].

This intricacy largely arises from the interfacial interactions between the nano entities and the matrix, as well as potential interfacial defects and localized strains. These insights not only illustrate the complexity of thermal behaviors at the nanoscale but also suggest meticulous consideration of multiscale and multi-interface effects in designing nanostructured materials and devices. For instance, an experimental study by Tong et al. found that the diffusion temperature, *Tm*(*D*), of nanostructured iron (Fe) was only around 573 K [40 – 43], while the corresponding bulk iron exhibited a diffusion temperature of 773 K under the same external conditions. This result explicitly reveals that nanocrystals can exhibit properties similar to their macroscopic counterparts at comparatively lower temperatures. Yet, data points derived from experiments are often discrete, making it challenging to establish generalized physical laws or models. Many theoretical calculation methods have been applied successfully to address this issue [4, 5, 8]. For example, Jesser and his

* Corresponding author. Tel.: +86-13786332495.
E-mail: *xust@chnu.edu.cn* (S.T. Xu)

colleagues validated through simulations that indium (In) nanocrystals start melting at temperatures lower than their bulk counterparts [43 – 47]. They attributed this primarily to changes in interactions among nearest neighbor atoms at the nanoscale [48 – 50]. Although several models have attempted to explain these phenomena, most existing models are limited to describing behaviors under specific conditions and fail to holistically explain the complex phenomena observed across different disciplines [51 – 54]. Therefore, a deeper integration of experimental and theoretical approaches is required to construct a more comprehensive and accurate model.

This study proposes a thermodynamic model describing the dependence of the melting point of nanocrystals on size and dimensionality from a cohesive energy perspective. This model is not only innovative theoretically but also validated in terms of accuracy by comparing it with available experimental data and simulation outcomes. This research enhances our understanding of the properties of nanomaterials and their potential applications. While the model is primarily developed for metallic nanocrystals, studies such as [19, 34] suggest that similar principles may apply to semimetal nanocrystals with certain parameter adjustments. Further research is needed to fully explore the model's applicability to nonmetal nanocrystals.

2. MODEL

Based on the cohesive energy of a metallic crystal, the relationship between cohesive energy $E_c(D)$ and bond energy $E_{bond}(\infty)$ can be written as follows [13]:

$$E_c(D) = \frac{\alpha N E_{bond}(D)}{8} + \frac{\alpha(n-N)}{2} E_{bond}(\infty), \quad (1)$$

where $E_c(D)$ is the cohesive energy of metallic nanocrystals and $E_{bond}(\infty)$ is the bond energy of bulk, $E_{bond}(D)$ represents the bond energy of a nanocrystal with size D, n represents the number of atoms in the nanocrystal, N represents the number of atoms in the bulk crystal, D represents the size or diameter of the nanocrystal, the number of interior atom forms bonds is parameter α. For the relationship between $E_{bond}(\infty)$ and $E_c(D)$, explicitly state that this conclusion is valid only if $E_{bond}(D) = E_{bond}(\infty)$ or if $E_{bond}(D)$ follows a particular form. Assuming that $E_{bond}(D)$ gradually approaches $E_{bond}(\infty)$ as D increases, we can derive the relationship $E_c(D) \propto E_{bond}(D)$. The expression of $E_{bond}(D)$ and $E_c(D)$ can be rewritten as:

$$E_c(D) = \frac{\frac{1}{2}\alpha(n-N)E_{bond}(\infty)}{1-\frac{\alpha N E_{bond}(\infty)}{8E_c(\infty)}}. \quad (2)$$

To account for the nanocrystals, suppose the atoms of nanoparticles are ideal spheres, the total number of atoms (n) is the ratio of the nanocrystals volume (V) to the volume of one atom (V_m), that is: $n = V/V_m$. The number of the surface atom N is the ratio of the nanocrystal surface area (A_m) to the effective surface area of one atom (A_{eff}). The contribution of one surface atom to the entire surface area is $A_m/4$, namely, $A_{eff} = A_m/4$. As the first order approximation, n is larger than N, and D trends to ∞. We are calculating the cohesive energy of one atom in bulk materials, where $n = 1$, and have derived the ideal model from Eq. 2 to Eq. 3. The cohesive energy of one atom of the bulk materials $E_c(\infty)$ can be written as:

$$E_c(\infty) = \frac{\alpha n}{2} E_{bond}(\infty). \quad (3)$$

Based on the previous idealized assumption that the atoms of the nanocrystals are perfect spheres and that all surface atoms contribute equally, this assumption provides the foundation for our subsequent derivations. Substituting Eq. 3 into Eq. 4, the cohesive energy of one atom can be expressed as:

$$\frac{E_c(D)}{E_c(\infty)} = \frac{1-\frac{N}{n}}{1-\frac{N}{4n}}. \quad (4)$$

According to the relationship between nanocrystals and dimensionalities d, A/V can be expressed as $A/V = D_0/D$, D_0 means the critical size at wich all atoms of crystal are located on its surface, and $D_0 = 2(3-d)h$, h means atomic diameter [22, 40]. Substituting the relation into Eq. 4, $E_c(D, d)/E_c(\infty)$ function can be approximated as:

$$\frac{E_c(D,d)}{E_c(\infty)} = \frac{1-4(3-d)h/3D}{1-(3-d)h/3D}, \quad (5)$$

where h is bond length and $d = 0$ for nanoparticles, $d = 1$ for nanowires and $d = 2$ for thin films [40]. Considering the relationship between $T_m(\infty)$ and $E_c(\infty)$, $T_m(\infty)$can be expressed as [41]:

$$\frac{T_m(D,d)}{T_m(\infty)} = \frac{1-4(3-d)h/3D}{1-(3-d)h/3D}. \quad (6)$$

Compared with chemisorption energy, Quyang declared that the role of elastic energy of deformation on the surface energy was rare [46]. So it is reasonable for us to use Eq. 6 to discuss the size and dimension dependence of $T_m(D, d)$ of metallic nanocrystals in detail.

3. RESULTS AND DISCUSSION

In this paper, the relevant data used in the model predictions are listed in Table 1 [48]. The effects of size and dimensionality on $Tm(D, d)/Tm(\infty)$ for Pb nanocrystals are exhaustively illustrated in Fig. 1, juxtaposed against experimental and theoretical data.

Table 1. The relevant data used in the model predictions [48]

h, nm	Pb	In	Au	Al	Bi	Pd	Ag	Sn
	0.35	0.31	0.27	0.25	0.46	0.28	0.32	0.29

We consider three nanocrystalline morphologies: nanoparticles (d =0), nanowires (d = 1), and nanofilms (d = 2). Evidently, for all forms, as the size D decreases, the $Tm(D, d)/Tm(\infty)$ value correspondingly diminishes. A closer inspection reveals two pronounced regimes: one where the value reduces as $D < 10$ nm and another which approximates a plateau for $D > 10$ nm. This trend can be attributed to the surge in the surface-to-volume ratio. For a given nanocrystal, while its volume remains constant, its surface area increases with its further division, leading to a decline in size D and a rise in the surface-to-volume ratio.

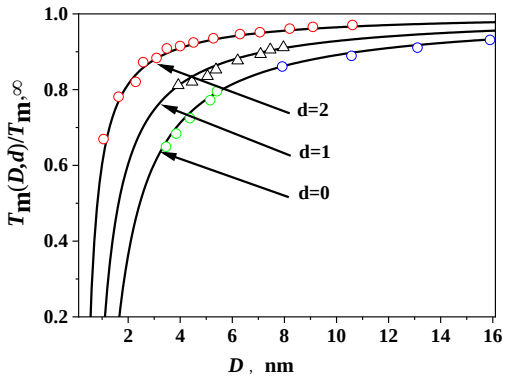

Fig. 1. The function $T_m(D, d)/T_m(\infty)$ of Pb versus D. The solid lines mean the model predictions in terms of Eq. 6 [4, 26, 49, 50]. The symbol ○[26] and ○[49], ○[4], △[50] are referred to experimental and simulation results for Pb nanoparticles, Pb nanowires, and Pb thin films, respectively

Allen delved deep into the characteristics of surface atoms, positing that as the size D of the nanocrystal shrinks, the energy states of surface atoms exceed those within the bulk [12]. This is primarily due to the augmented number of broken bonds, thereby amplifying interfacial energy [48]. Typically, the physicochemical properties of nanocrystals are predominantly governed by their surface strain. In macro-crystals, atoms can often achieve full coordination with their counterparts. However, on the nanoscale, the lack of complete coordination for surface atoms results in surface strain. This strain becomes more pronounced with diminishing size D. Yet, when the nanoparticle size approaches that of individual atoms or molecules, adjustments might occur in the inter-atomic distances to accommodate the new coordination environment. The attenuation of surface strain allows atoms greater freedom, leading to an upswing in their thermal vibration amplitude. Qi's model elucidated that the $Tm(D)$ and D relationship remains linear across a broad size spectrum but begins to deviate when $D < 10$ nm [13, 29]. Relative to this model, our simulation data is more congruent with experimental findings at smaller scales.

Considering the effects at the nanoscale, Li derived a model that describes the relationship between $\beta(D)$ and size D [22], which, specifically, predicts a linear correlation between $\beta(D)$ and D [39]. Combining equation $T_m(D)/T_m(\infty) = 1 - \beta/zD$ and Eq. 6 [11], yields the expression for

$$\beta(D) = 1 + \frac{3hd}{D} . \quad (7)$$

However, data in Fig. 2 illustrates a non-linear relationship when comparing $\beta(D)$ with $1/D$. Based on these observations and analysis, we can assert that the size dependency of $T_m(D)$ is primarily influenced by its surface-to-volume ratio and the variation in surface interfacial energy, an effect that is particularly pronounced when D is less than 10 nm. The model assumes that within a certain size range, particularly when DDD approaches the nanoscale, due to the enhancement of surface effects and the reduction of volume effects, the relationship between Tm(D)/Tm(∞) and 1/D exhibits nonlinear characteristics.

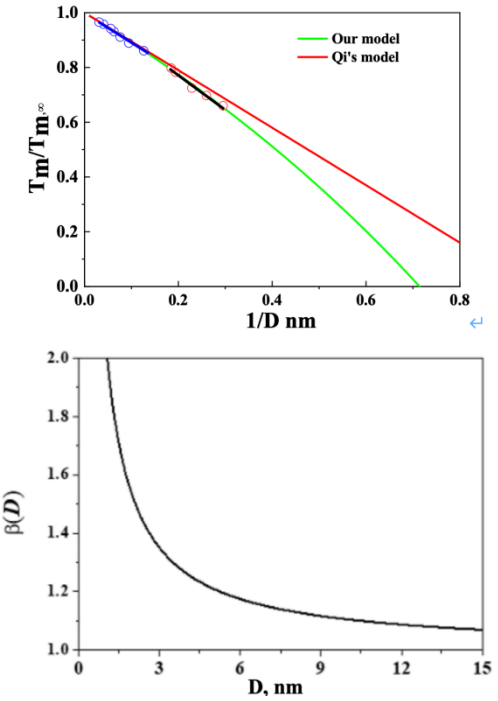

Fig. 2. $T_m(D)/ T_m(\infty)$ of Pb nanoparticles as a function of inverse D relation with Eq. 7. The insertion diagrams are shape factor $\beta(D)$ function versus D. The symbols ○[26] and ○[50] come from experimental and theoretical results for Pb NPs

To delve deeper into size effects at the nanoscale, we precisely fit experimental data [49] with simulation data [46] in Fig. 2. The blue curve has a slope of -1.15, whereas the black curve exhibits a slope of -1.23. Notably, within the larger size regime ($D > 10$ nm), the blue, green, and red curves almost overlap, manifesting the high consistency of various models with experimental data at this scale. Observing the range where $D > 10$ nm, the trend aligns well with the models of Li and Qing [13, 22]. However, in the size domain of $D < 10$ nm, the black curve is insignificant alignment with the slope change in our model, further corroborating that our model provides a more scientific explanation for the relationship between $T_m(D)$ and D at the microscale. It's worth emphasizing that although the overall trend in slope variations is somewhat analogous across models, the rate of slope change in our model is distinctly slower than that of Li's or Nanda's models [22, 51]. A juxtaposition with Li's model reveals that, on the scale where $D < 10$ nm [22], our model has a notably superior fit with experimental data.

Numerous studies have unambiguously shown that with the reduction in nanoscale size, associated slopes also progressively decrease. Li's model, while addressing energy variations from a Gibbs free energy standpoint, might not have adequately considered the influence of broken bonds [22]. Further research by Hornyak confirms that as the dimension D diminishes, the relative bond length on the surface increases, leading to surface atoms possessing energy levels surpassing those of inner atoms [54]. This results in an amplified vibrational amplitude of surface atoms at equivalent temperatures due to the heightened energy levels. As size continues to shrink, this effect becomes even more pronounced [52]. The surface free energy γ_{ls} is largely regulated by the number of broken

bonds and serves as a critical metric in assessing the energy stability of nanocrystals. Moreover, the characteristics of surface atoms might further influence surface energy differences, denoted as $\Delta\gamma_{sv}$. A deep dive into $\Delta\gamma_{sv}$ will enhance our comprehension of the alterations in temperature gradient $\Delta T(D)$ and the underlying melting behaviors. As pointed out by Quyang's team, $\Delta\gamma_{sv}$ of nanoparticle is affected by two main factors: structural differences caused by surface strain and chemical changes due to broken bonds [47]. Within smaller scales, the trend in ΔT (D) becomes more prominent and directly correlates with the A/V ratio. The surface strain further precipitates a decline in melting point. From an integrative analysis, it can be deduced that on smaller scales, changes in ΔT (D) induced by surface strain are even more significant than variations in the A/V ratio.

Additionally, as illustrated in Fig. 3, we have evaluated size and dimensional effects across different nanocrystals to ascertain the broad applicability of Eq. 6. The outcomes reveal that whether it's Au, Al, Bi, Ag, Sn, or In nanoparticles, our simulation results align remarkably well with either experimental or theoretical data. In conjunction with Fig. 1, this high level of consistency further substantiates the accuracy and universality of Eq. 6 in depicting the relationship between $Tm(D)/Tm(\infty)$ and nanoscale dimensions.

4. CONCLUSIONS

In the field of nanomaterials research, we have proposed a novel thermodynamic model aimed at exploring in-depth the relationship between the melting point of nanocrystals and their size and dimensions. Through a comprehensive assessment of various materials such as Au, Al, Bi, Ag, Sn, and In, our model's predicted results align closely with existing experimental data and theoretical simulations, thus validating the reliability and accuracy of the model. Within larger size scales, we observe that the relationship between melting point and particle size is generally linear, but when the size decreases below 10 nm, this relationship begins to exhibit a non-linear trend, emphasizing the significance of size effects at the nanoscale.

More importantly, our study reveals that as the size of nanoparticles decreases, the dependence of melting point on size further intensifies, closely associated with the changing energy of surface atoms. This finding provides valuable insights into understanding the unique melting point characteristics of nanomaterials. It not only deepens our understanding of the mechanisms behind the variation in melting points of nanomaterials but also offers valuable information for the design of future electronic devices and other high-tech applications. In summary, our research lays a solid foundation for the field of nanomaterials science and opens up new perspectives and possibilities for materials design and optimization.

Acknowledgments

The Major Foundation of Educational Commission of Anhui Province (2022AH040068); Horizontal scientific research project of Huaibei Normal University (No.22100281); The Natural Science Foundation of Education Committee of Anhui Province (No. 2024AH051673).

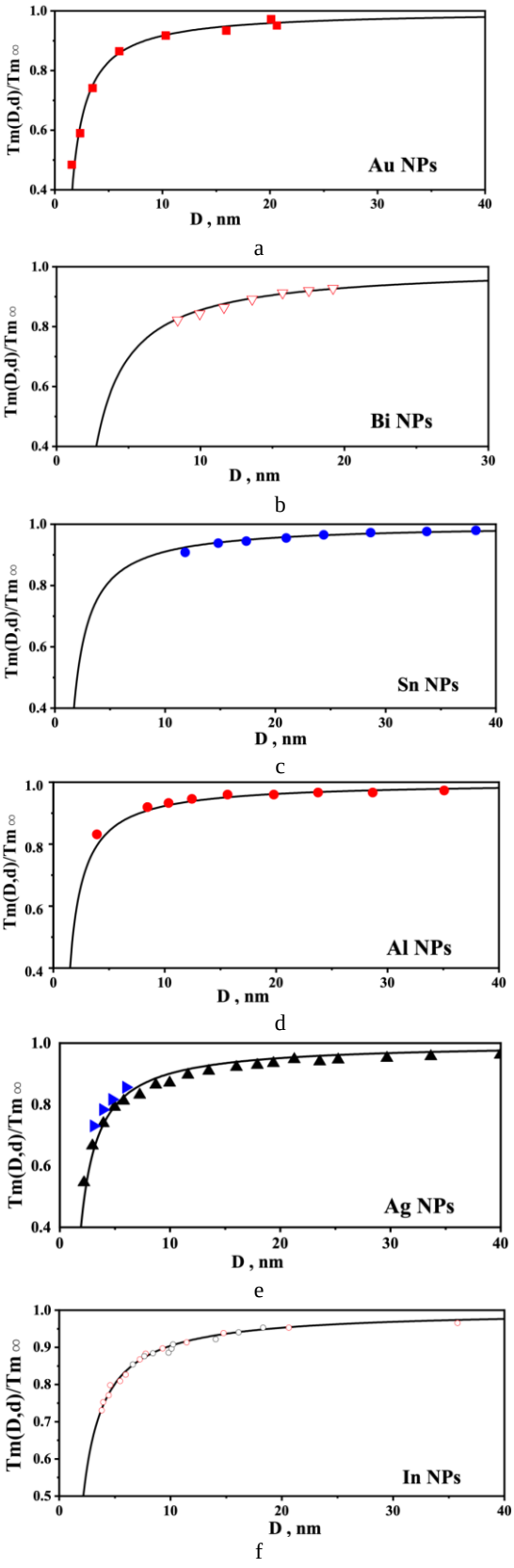

Fig. 3. $T_m(D)/T(\infty)$ of Au, Al, Bi, Ag, Sn, In nanoparticles in relations with Eq. 7 [23, 24, 26, 32, 49, 51 – 53], The symbols ■ [23], ● [26], △ [24] and ▲ [51] related with experimental data and ▲ [52], ● [53], ○ [49] ○ [32] related with theoretical simulation results

REFERENCES

1. **Li, Y., Li, Z., Misra, R.P., Liang, C., Gillen, A.J., Zhao, S., Abdullah, J., Laurence, T., Fagan, J.A., Aluru, N., Blankschtein, D., Noy, A.** Molecular Transport Enhancement in Pure Metallic Carbon Nanotube Porins *Nature Materials* 23 2024: pp. 1123 – 1130. https://doi.org/10.1038/s41563-024-01925-w
2. **Thompson, A.P., Aktulga, H.M., Berger, R., Bolintineanu, D.S., Brown, W.M., Crozier, P.S., in 't Veld, P.J., Kohlmeyer, A., Moore, S.G., Nguyen, T.D., Shan, R., Stevens, M.J., Tranchida, J., Trott, C., Plimpton, S.J.** LAMMPS - A Flexible Simulation Tool for Particle-Based Materials Modeling at the Atomic, Meso, and Continuum Scales *Computer Physics Communications* 271 2022: pp. 108171. https://doi.org/10.1016/j.cpc.2021.10817
3. **Hicks, J.M., Yao, Y.C., Barber, S., Neate, N., Watts, J.A., Noy, A., Rawson, F.J.** Electric Field Induced Biomimetic Transmembrane Electron Transport Using Carbon Nanotube Porins *Small* 17 (32) 2021: pp. 2102517. https://doi.org/10.1002/smll.202102517
4. **Epsztein, R., Duchanois, R.M., Ritt, C.L., Noy, A., Elimelech, M.** Towards Single-Species Selectivity of Membranes with Subnanometre Pores *Nature Nanotechnology* 15 2020: pp. 426 – 436. https://doi.org/10.1038/s41565-020-0713-6
5. **Noy, A., Park, H.G., Fornasiero, F., Holt, J.K., Grigoropoulos, C.P., Bakajin, O.** Nanofluidics in Carbon Nanotubes *NanoToday* 2 (6) 2007: pp. 22 – 29. https://doi.org/10.1016/S1748-0132(07)70170-6
6. **Guisbiers, G., Khanal, S., Ruiz-Zepeda, F., de la Puente, J.R., José-Yacaman, M.** Cu–Ni Nano-Alloy: Mixed, Core–Shell or Janus Nano-Particle? *Nanoscale* 6 (24) 2014: pp. 14630 – 14635. https://doi.org/10.1039/C4NR05739B
7. **Pavan, L., Baletto, F., Novakovic, R.**, Multiscale Approach for Studying Melting Transitions in CuPt Nanoparticles *Physical Chemistry Chemical Physics* 17 (42) 2015: pp. 28364 – 28371. https://doi.org/10.1039/C5CP01096A
8. **Li, Z., Misra, R.P., Li, Y., Yao, Y.C., Zhao, S., Zhang, Y., Chen, Y., Blankschtein, D., Noy, A.** Breakdown of the Nernst-Einstein Relation in Carbon Nanotube Porins *Nature Nanotechnology* 18 (2) 2023: pp. 177 – 183. https://doi.org/10.1038/s41565-022-01276-0
9. **Ferrando, R., Jellinek, J., Johnston, R.L.** Nanoalloys: from Theory to Applications of Alloy Clusters and Nanoparticles *Chemical Reviews* 108 (3) 2008: pp. 845 – 910. https://doi.org/10.1021/cr040090g
10. **Sankaranarayanan, S.K., Bhethanabotla, V.R., Joseph, B.** Molecular Dynamics Simulation Study of the Melting of Pd-Pt Nanoclusters *Physical Review B* 71 (19) 2005: pp. 195415. https://doi.org/10.1103/PhysRevB.71.195415
11. **Remhof, A., Westphalen, A., Theis-Bröhl, K., Grabis, J., Nefedov, A., Toperverg, B., Zabel, H.,** Magnetic Nanostructures. Springer Series in Materials Science, vol 94. Springer, Berlin, Heidelberg. 2007: pp. 65 – 96. https://doi.org/10.1007/978-3-540-49336-5_6
12. **Aluru, N.R., Aydin, F., Bazant, M.Z., Blankschtein, D., Brozena, A.H., de Souza, J.P., Zhang, Z.** Fluids and Electrolyte Under Confinement in Single-Digit Nanopores *Chemical Reviews* 123 (6) 2023: pp. 2737 – 2831. https://doi.org/10.1021/acs.chemrev.2c00155
13. **Qi, W., Wang, M.** Size and Shape Dependent Melting Temperature of Metallic Nanoparticles *Materials Chemistry and Physics* 88 (2 – 3) 2004: pp. 280 – 284. https://doi.org/10.1016/j.matchemphys.2004.04.026
14. **Tunuguntla, R.H., Allen, F.I., Kim, K., Belliveau, A., Noy, A.** Ultrafast Proton Transport in Sub-1-nm Diameter Carbon Nanotube Porins *Nature Nanotechnology* 11 2016: pp. 639 – 644. https://doi.org/10.1038/nnano.2016.43
15. **Hicks, J.M., Yao, Y.C., Barber, S., Neate, N., Watts, J.A., Noy, A., Rawson, F.J.** Electric Field Induced Biomemetic Transmembrane Electron Transport Using Carbon Nanotube Porins *Small* 17 (32) 2021: pp. 2102517. https://doi.org/10.1002/smll.202102517
16. **Zhao, M., Jiang, Q.** Melting and Surface Melting of Low-Dimensional in Crystals *Solid State Communications* 130 (1 – 2) 2004: pp. 37 – 39. https://doi.org/10.1016/j.ssc.2004.01.016
17. **Yang, C., Xiao, M., Li, W., Jiang, Q.** Size Effects on Debye Temperature, Einstein Temperature, and Volume Thermal Expansion Coefficient of Nanocrystals *Solid State Communications* 139 (4) 2006: pp. 148 – 152. https://doi.org/10.1016/j.ssc.2006.05.035
18. **Verduci, R., Creazzo, F., Tavella, F., Abate, S., Ampelli, C., Luber, S., Perathoner, S., D'Angelo, G.** Water Structure in the First Layers on TiO_2: A Key Factor for Boosting Solar-Driven Water-Splitting Performances *Journal of the American Chemical Society* 146 2024: pp. 18061 – 18073. https://doi.org/10.1021/jacs.4c05042
19. **Cano-Casanova, L., Ansó-Casaos, A.** Surface -Enriched Boron-doped TiO_2 Nano-Particles as Photocatalysts for Propene Oxidation *ACS Applied Nano Materials* 5 (9) 2022: pp. 12527 – 12539. https://doi.org/10.1021/acsanm.2c02217
20. **Yang, C.C., Li, S.** Investigation of Cohesive Energy Effects on Size-Dependent Physical and Chemical Properties of Nanocrystals *Physical Review B* 75 (16) 2007: pp. 165413. https://doi.org/10.1103/PhysRevB.75.165413
21. **Ash, B., Amir, A., Bar-Sinai, Y., Oreg, Y., Imry, Y.** Thermal Conductance of One-Dimensional Disordered Harmonic Chains *Physical Review B* 101 (12) 2020: pp. 121403. https://doi.org/10.1103/PhysRevB.101.121403
22. **Chen, T.D., Ma, Y.L., Fu, X.L., Li, M.** A Comprehensive Understanding of the Melting Temperature of Nanocrystals: Implications for Catalysis *ACS Applied Nano Materials* 3 2020: pp. 1583 – 1591. https://doi.org/10.1021/acsanm.9b02365
23. **Dick, K., Dhanasekaran, T., Zhang, Z., Meisel, D.** Size-Dependent Melting of Silica-Encapsulated Gold Nanoparticles *Journal of The American Chemical Society* 124 (10) 2002: pp. 2312 – 2317. https://doi.org/10.1021/ja017281a
24. **Samanta, B., Morales-García, Á., Illas, F., Goga, N., Anta, J.A., Calero, S., Toroker, M.C., Hutter, A.B., Libisch, F., Toroker, M.C.** Challenges of Modeling Nanostructured Materials for Photocatalytic Water Splitting *Chemical Society Reviews* 51 (9) 2022: pp. 3794 – 3818. https://doi.org/10.1039/d1cs00648g
25. **Lai, S., Carlsson, J., Allen, L.** Melting Point Depression of Al Clusters Generated During the Early Stages of Film Growth: Nanocalorimetry Measurements *Applied Physics Letters* 72 (9) 1998: pp. 1098 – 1100. https://doi.org/10.1063/1.120946
26. **Tan, C., Cao, X., Wu, X.J., He, Q., Yang, J., Zhang, X., Chen, J.Z., Zhao, W., Han, S.K., Nan, G.H., Sindoro, M., Zhang, H.** Recent Advances in Ultrathin Two-Dimensional Nanomaterials *Chemical Reviews* 117 (10) 2017: pp. 6225 – 6331.

https://doi.org/10.1021/acs.chemrev.6b00558
27. **Lu, H., Jiang, Q.** Size-dependent Surface Energies of Nanocrystals *The Journal of Physical Chemistry B* 108 (18) 2004: pp. 5617 – 5619. https://doi.org/10.1021/jp0366264
28. **Miao, L., Bhethanabotla, V.R., Joseph, B.** Melting of Pd Clusters and Nanowires: A Comparison Study Using Molecular Dynamics Simulation *Physical Review B* 72 (13) 2005: pp. 134109. https://doi.org/10.1103/PhysRevB.72.134109
29. **Qi, W.** Size Effect on Melting Temperature of Nanosolids *Physica B: Condensed Matter* 368 (1 – 4) 2005: pp. 46 – 50. https://doi.org/10.1016/j.physb.2005.06.035
30. **Abdul Nasir, J., Munir, A., Ahmad, N., Haq, T.U., Khan, Z., Rehman, Z.** Photocatalytic Z-Scheme Overall Water Splitting: Recent Advances in Theory and Experiments *Advanced Materials* 33 (52) 2021: pp. 2105195. https://doi.org/10.1002/adma.202105195
31. **Shi, Z., Ge, Y., Yun, Q., Zhang, H.** Two-Dimensional Nanomaterial-Templated Composites *Accounts of Chemical Research* 55 (24) 2022: pp. 3581 – 3593. https://doi.org/10.1021/acs.accounts.2c00579
32. **Barnard, A.S., Zapol, P.** A Model for the Phase Stability of Arbitrary Nanoparticles as A Function of Size and Shape *The Journal of Chemical Physics* 121 (9) 2004: pp. 4276 – 4283. https://doi.org/10.1063/1.1775770
33. **Fan, F.R., Wang, R., Zhang, H., Wu, W.** Emerging Beyond-Graphene Elemental 2D Materials for Energy and Catalysis Applications *Chemical Society Reviews* 50 (19) 2021: pp. 10983 – 11031. https://doi.org/10.1039/C9CS00821G
34. **Gan, S., Zhao, H., Quan, X.** Two-dimensional MoS_2: A Promising Building Block for Biosensors *Biosens Bioelectron* 89 2017: pp. 56 – 71. https://doi.org/10.1016/j.bios.2016.03.042
35. **Samsonov, V., Sdobnyakov, N.** A Thermodynamic Approach to Mechanical Stability of Nanosized Particles *Open Physics* 1 (2) 2003: pp. 344 – 354. https://doi.org/10.2478/BF02476301
36. **Zhao, M., Zheng, W., Li, J., Wen, Z., Gu, M., Sun, C.Q.** Atomistic Origin, Temperature Dependence, and Responsibilities of Surface Energetics: An Extended Broken-Bond Rule *Physical Review B* 75 (8) 2007: pp. 085427. https://doi.org/10.1103/PhysRevB.75.085427
37. **Jiang, Q., Shi, H., Zhao, M.** Free Energy of Crystal–Liquid Interface *Acta Materialia* 47 (7) 1999: pp. 2109 – 2112. https://doi.org/10.1016/S1359-6454(99)00085-3
38. **Trelin, A., Skvortsova, A., Olshtrem, A., Chertopalov, S., Mares, D., Lapcak, L., Vondracekt, M., Sajdl, P., Jerabek, V., Maixner, J., Lancok, J., Sofer, Z., Regner, J., Kolska, Z., Svorcik, V., Lyutakov, O.** Surface-Enhanced Raman Spectroscopy and Artificial Neural Networks for Detection of MXene Flakes' Surface Terminations *The Journal of Physical Chemistry C* 128 (16) 2024: pp. 6780 – 6787. https://doi.org/10.1021/acs.jpcc.4c01273
39. **Tian, Y., Boulatov, R.** Comment on T. Stauch, A. Dreuw, "Stiff-stilbene Photoswitch Ruptures Bonds not by Pulling but by Local Heating" *Physical Chemistry Chemical Physics* 18 (38) 2016: pp. 26990 – 26993. https://doi.org/10.1039/C6CP04696G
40. **Zhang, Z., Li, J.C., Jiang, Q.** Modelling for Size-Dependent and Dimension-Dependent Melting of Nanocrystals *Journal of Physics D: Applied Physics* 33 (20) 2000: pp. 2653 – 2656. https://doi.org/10.1088/0022-3727/33/20/318
41. **Shreiber, D., Jesser, W.** Size Dependence of Lattice Parameter for SixGe1− x Nanoparticles *Surface Science* 600 (19) 2006: pp. 4584 – 4590. https://doi.org/10.1016/j.susc.2006.07.026
42. **Zhu, Y., Lian, J., Jiang, Q.** Modeling of the Melting Point, Debye Temperature, Thermal Expansion Coefficient, and the Specific Heat of Nanostructured Materials *Journal of Physical Chemistry C* 113 (39) 2009: pp. 16896 – 16900. https://doi.org/10.1021/jp902097f
43. **Jesser, W., Shneck, R., Gile, W.** Solid-liquid Equilibria in Nanoparticles of Pb-Bi Alloys *Physical Review B* 69 (14) 2004: pp. 144121. https://doi.org/10.1103/PhysRevB.69.144121
44. **Jiang, Q., Zhao, D., Zhao, M.** Size-dependent Interface Energy and Related Interface Stress *Acta Materialia* 49 (16) 2001: pp. 3143 – 3147. https://doi.org/10.1016/S1359-6454(01)00232-4
45. **Pellegrini, G., Mattei, G., Mazzoldi, P.** Finite Depth Square Well Model: Applicability and Limitations *Journal of Applied Physics* 97 (7) 2005: pp. 073706. https://doi.org/10.1063/1.1868875
46. **Omar, M.** Structural and Thermal Properties of Elementary and Binary Tetrahedral Semiconductor Nanoparticles *International Journal of Thermophysics* 37 (1) 2016: pp. 11. https://doi.org/10.1007/s10765-015-2026-9
47. **Ouyang, G., Tan, X., Cai, M., Yang, G.** Surface Energy and Shrinkage of a Nanocavity *Applied Physics Letters* 89 (18) 2006: pp. 183104. https://doi.org/10.1063/1.2374808
48. **Winter, M.** WebElements Periodic Table: the Periodic Table on the Web. 2015.
49. **Unruh, K., Huber, T., Huber, C.** Melting and Freezing Behavior of Indium Metal in Porous Glasses *Physical Review B* 48 (12) 1993: pp. 9021. https://doi.org/10.1103/PhysRevB.48.9021
50. **Zhang, H.** Ultrathin Two-Dimensional Nanomaterials *ACS Nano* 9 (10) 2015: pp. 9451 – 9469. https://doi.org/10.1021/acsnano.5b05040
51. **Nanda, K., Sahu, S., Behera, S.** Liquid-drop Model for the Size-Dependent Melting of Low-Dimensional Systems *Physical Review A* 66 (1) 2002: pp. 013208. https://doi.org/10.1103/PhysRevA.66.013208
52. **Jiang, Q., Yang, C.** Size Effect on the Phase Stability of Nanostructures *Current Nanoscience* 4 (2) 2008: pp. 179 – 200. https://doi.org/10.2174/157341308784340949
53. **Jiang, Q., Shi, H., Zhao, M.** Melting Thermodynamics of Organic Nanocrystals *The Journal of Chemical Physics* 111 (5) 1999: pp. 2176 – 2180. https://doi.org/10.1063/1.479489
54. **Hornyak, G.L., Tibbals, H.F., Dutta, J., Moore, J.J.**, *Introduction to Nanoscience and Nanotechnology*. CRC Press: 2008. https://doi.org/10.1201/9781420047806